

Kent Academic Repository

Full text document (pdf)

Citation for published version

Betancourt, J.E. and Marti n-Hidalgo, M. and Gubala, V. and Rivera, J.M. (2009) Solvent-induced high fidelity switching between two discrete supramolecules. *Journal of the American Chemical Society*, 131 (9). pp. 3186-3188. ISSN 0002-7863.

DOI

<https://doi.org/10.1021/ja809612d>

Link to record in KAR

<http://kar.kent.ac.uk/45245/>

Document Version

Author's Accepted Manuscript

Copyright & reuse

Content in the Kent Academic Repository is made available for research purposes. Unless otherwise stated all content is protected by copyright and in the absence of an open licence (eg Creative Commons), permissions for further reuse of content should be sought from the publisher, author or other copyright holder.

Versions of research

The version in the Kent Academic Repository may differ from the final published version.

Users are advised to check <http://kar.kent.ac.uk> for the status of the paper. **Users should always cite the published version of record.**

Enquiries

For any further enquiries regarding the licence status of this document, please contact:

researchsupport@kent.ac.uk

If you believe this document infringes copyright then please contact the KAR admin team with the take-down information provided at <http://kar.kent.ac.uk/contact.html>

Published in final edited form as:

J Am Chem Soc. 2009 March 11; 131(9): 3186–3188. doi:10.1021/ja809612d.

Solvent-Induced High Fidelity Switching Between two Discrete Supramolecules

José E. Betancourt, Mariana Martín-Hidalgo, Vladimir Gubala, and José M. Rivera*

Department of Chemistry, University of Puerto Rico, Río Piedras Campus, Río Piedras, Puerto Rico 00931

Switches are crucial elements for the construction of complex molecular machinery. There are numerous examples of supramolecular systems that can interconvert between two or more distinct states via photochemical, electrochemical or chemical stimuli.¹ However, most examples of switching self-assembled supramolecules involve systems in which the structures alternate between two extreme states. Specifically, a discrete and well-defined supramolecule can be induced to disassemble into its constituent subunits^{2, 3} or to form higher-order and ill-defined aggregates (e.g. self assembled polymers, gels).⁴ On the other hand, switching between two discrete and well-defined assemblies of relatively high molecularity (> 8 subunits), which are robust enough to form with high fidelity, yet sensitive enough to switch induced by subtle changes in the environment remains a challenge.⁵ Here we show the reversible switching between a self-assembled hexadecamer (H) and an octamer (O) with high fidelity (e.g. from ~100% H to ~100% O) by simply changing the solvent from CD₃CN to CDCl₃ respectively. Our results suggest that the switching is triggered by an unprecedented indirect mechanism resulting from a subtle interplay between the lower activity of potassium iodide in CDCl₃ and the steric crowding within the supramolecule.

Lipophilic guanosine derivatives self-assemble into planar hydrogen-bonded tetramers (G-tetrads, Figure 1), which further stack to form supramolecules known as G-quadruplexes.⁶ We have demonstrated that the supramolecular properties of 8-phenyl-2'-deoxyguanosine derivatives (8PhGs), such as their thermal stability and their selectivity for binding metal cations, can be modulated by the presence of a *para*- (**pAGi**) or a *meta*- (**mAGi**) acetyl group.⁷ In organic media and under identical conditions, **pAGi** forms an octamer whereas **mAGi** forms a hexadecamer. In fact, the 8-(*m*-acetylphenyl)- moiety induces the formation of hexadecamers very reliably, in both organic and aqueous media and even with large, sterically demanding groups like dendrons attached to the sugar ring.⁸

Similar to **mAGi**, titration of a solution of the novel 8-(*m*-ethoxycarbonylphenyl)-2'-deoxyguanosine (**mECGi**) with KI in CD₃CN shows initially the formation of an octamer (at low [KI], Figure 2a). The eventual addition of more KI (0.5 eq.) leads to the formation of a hexadecamer with high fidelity (Figure 2b).⁹ The ¹H NMR spectrum shows the characteristic double set of signals corresponding to two pairs of tetrads (N¹H) in different chemical environments (Figure 2b). The 2D NOESY spectrum also shows signature cross peaks that are characteristic of the hexadecamer (**mAGi**)₁₆ (Figure S8).⁹ DOSY NMR experiments in CD₃CN gives a molecular translational coefficient (D) value of $(6.05 \pm 0.15) \times 10^{-10} \text{ m}^2 \text{ s}^{-1}$ at 298 K, corresponding to a hydrodynamic radius (r_H) of 10.6 Å.^{10, 11} Similarly, vapor

jmrivortz@mac.com .

 Supporting Information Available Detailed synthetic procedures, characterization for all new compounds, experimental protocols and NMR data. This material is available free of charge via the Internet at <http://pubs.acs.org>.

pressure osmometry (VPO) measurements of **mECGi** in CD₃CN gives a molecular weight of 9,192 Da, which is consistent to the value expected for a hexadecamer¹².

Although similar, the resulting hexadecamers formed by **mECGi** and **mAGi** have important differences. Dose-response curves show that the proportion of (**mECGi**)₁₆ is higher than that of (**mAGi**)₁₆ at the corresponding values of log [KI] (Figure 3a).¹³ Analysis of such curves yield Hill coefficients (n_H) of 5.4 ± 0.4 for (**mECGi**)₁₆ and 5.0 ± 0.6 for (**mAGi**)₁₆, suggesting that the formation of the former might be slightly more cooperative.^{9, 13, 14} On the other hand, (**mECGi**)₁₆ ($T_m = 323.5$ K) is thermally less stable than (**mAGi**)₁₆ ($T_m = 329.2$ K) (Figure 3b). NMR studies show that the high level of cooperativity in the assembly and disassembly of these systems result from a very close-packing of the subunits.¹⁵ Thus, the increased steric repulsion induced by the larger ethoxy groups destabilizes (**mECGi**)₁₆.

Surprisingly, and unlike **mAGi** that consistently forms a hexadecamer, changing the solvent to CDCl₃ shifts the equilibrium from the hexadecamer (**mECGi**)₁₆ towards the octamer (**mECGi**)₈ (Figures 2e, 4 a–b). In solutions of (**mECGi**)₁₆ in CD₃CN with increasing proportions of CDCl₃ it is possible to detect the presence of the octamer (**mECGi**)₈ when the proportions of each solvent is 1:1 (Figure 2c). Beyond this point the amount of octamer increases until it becomes the main species (Figure 2d–e). The fact that the main species in Figure 2e shows only one set of signals indicates the formation of a D₄-symmetrical octamer. The results of 2D NOESY (Figure S9) and DOSY experiments in CDCl₃ are also consistent with the formation of an octamer, with the latter giving a $D = (6.57 \pm 0.12) \times 10^{-10} \text{ m}^2 \text{ s}^{-1}$ at 298 K, which corresponds to a hydrodynamic radius (r_H) of 6.13 Å.⁹

We hypothesized that a change in the activity of the potassium cation, induced by a change in solvent, is at the heart of this phenomenon. But, how does changing the solvent decreases the activity? In a solvent of low relative permittivity, such as chloroform, KI is expected to exist primarily as a solvated contact ion pairs with practically no “free” solvated ions in solution and the energy of such contact ion pair is similar to that of a covalent bond.¹⁶ On the other hand, in a solvent of intermediate relative permittivity, such as acetonitrile, KI is expected to exist as a mixture of solvated contact ion pair and free solvated ions that are more available for complexation.⁹

To further support the hypothesis of the lower potassium cations activity, we tested two independent ways to reduce it; by adding a competitive cationophore (i.e. [2.2.2]-cryptand)⁴ and by using a smaller anion (i.e. from I⁻ to Cl⁻).¹⁷ Using the [2.2.2]-cryptand enables the switching of both (**mECGi**)₁₆ and (**mAGi**)₁₆ to their respective octamers (Figure 4c, Figures S11–12).⁹ Similarly, when KCl is used as the source of potassium, the equilibria in CD₃CN for both **mECGi** and **mAGi** are displaced away from the hexadecamer and towards the octamer, leading to a mixture of assemblies (i.e. lower fidelity, Figure S6).⁹ Unfortunately, the selective switching of (**mECGi**)₁₆ over (**mAGi**)₁₆ is not obtained under any of these conditions, which underscores the advantage of using the solvent as the triggering mechanism.

So far we have established that the differential switching of (**mECGi**)₁₆ over (**mAGi**)₁₆ is related to the lower stability of the former and the lower potassium cations activity. At higher potassium cation activities, the formation of the hexadecamer is favored over the formation of an octamer. After the stimulus, the driving force for the decay (ΔG_d) from H to O can be expressed mathematically as: $\Delta G_d = \mu_O - \mu_H$, where μ_O and μ_H are the chemical potentials of the octamer and the hexadecamer respectively (Figure 4).¹⁸ Only when ΔG_d is negative ($\mu_H > \mu_O$) will the decay occur spontaneously. The μ_H is affected by intrinsic parameters, such as the structural features of the subunits, and by extrinsic parameters such as the solvent, temperature, and the activity of the “free” solvated potassium cations in solution ($a_{K, S}$). Decreasing the $a_{K, S}$ increases μ_H , relative to μ_O , as a direct consequence of the increased chemical potential

of potassium cations inside the hexadecamer ($\mu_{K, H}$), relative to the “free” solvated cations in solution ($\mu_{K, S}$). This concentration gradient ($\Delta\mu_K$) induces a spontaneous net flow of potassium cations away from the hexadecamer as described by $\Delta\mu_{K, S} = \mu_{K, S2} - \mu_{K, S1} = RT \ln (a_{K, S2}/a_{K, S1})$, where $a_{K, S1}$ and $a_{K, S2}$ are the activities of free solvated potassium cations, with 1 and 2 referring respectively to the states before and after the stimulus has been applied.¹⁸

Before the stimulus, the system is at equilibrium for both **mECGi** and **mAGi**, therefore $\mu_{K, H1} = \mu_{K, S1}$ and $\mu_{H1} < \mu_{O1}$. Immediately after the stimulus $\mu_{K, H1} > \mu_{K, S2}$ (with $a_{K, S2} < a_{K, S1}$) until a second equilibrium is attained, where $\mu_{K, H2} = \mu_{K, S2}$. Since $a_{K, S2} < a_{K, S1}$ it follows that $\mu_{H2} > \mu_{H1}$ (Figure 4). When the stimulus consists on switching the solvent (CD_3CN to $CDCl_3$), for **mAGi**, $\mu_{H2} < \mu_{O2}$ so the hexadecamer remains, but for **mECGi**, $\mu_{H2} > \mu_{O2}$, therefore the hexadecamer decays to an octamer (Figure 4b). What pushes μ_{H2} over the threshold for **mECGi**, relative to **mAGi**, is the increased steric crowding within the supramolecule described earlier.

Interestingly, the switching process is not instantaneous and it takes approximately 110 min for full interconversion, showing a short-term memory effect (Figure S10).¹⁹ Analysis of the kinetic data shows that the dissociation process from the hexadecamer to the octamer is first order with respect of the hexadecamer ($t_{1/2} = 19.25$ min).⁹ EXSY NMR experiments revealed that the exchange between monomeric subunits and (**mECGi**)₁₆ occurs only with the outer tetrads.²⁰ These results support a mechanism of interconversion in which the hexadecamer peels off the subunits in the two outer tetrads leaving behind an octamer, which were formerly the inner tetrads (Scheme 1). Because the cation exchange is at least three orders of magnitude faster than subunit exchange, we propose that the decay is mediated by the transient formation of a metastable hexadecamer (H^* , Scheme 1) leading to the eventual formation of the octamer.
21, 22

Since hydrophilic versions of 8PhGs can self-assemble isostructurally in aqueous media,^{8a} the principles reported could be applied to the development of supramolecular nanoprobe for cellular studies. Given that the interior of cells is remarkably heterogeneous, such probes could be developed to dynamically switch their constitution as a function of specific cellular environs. Such switching will encompass changes in size, shape and the number of functional groups at the surface of the supramolecule, we expect that the resulting probes will open new windows into the interior of cells. The results of such studies will be reported in due course.

Supplementary Material

Refer to Web version on PubMed Central for supplementary material.

Acknowledgments

We thank NIH-SCoRE (2506GM08102) for financial support. J.E.B. and M.M.H thank the Alfred P. Sloan Foundation, NSF-IFN-EPSCoR (01A-0701525), PRIDCO and NIH-RISE (2R25GM61151) for graduate fellowships. We also thank Stephanie Rivera for technical help, Prof. Rafael Arce and Mrs. Marilyn García (UPRRP) for helpful discussions.

References

- (1). (a) Balzani, V.; Credi, A.; Venturi, M. *Molecular Devices and Machines - A Journey into the Nano World*. Wiley-VCH; Weinheim: 2003. (b) Feringa, BL. *Molecular Switches*. Wiley-VCH; Weinheim: 2001. (c) Feringa BL. *J. Org. Chem* 2007;72:6635–6652. [PubMed: 17629332]
- (2). Balzani V, Credi A, Venturi M. *Proc. Natl. Acad. Sci. U.S.A* 2002;99:4814–4817. [PubMed: 11891279]
- (3). Moon K, Kaifer AE. *J. Am. Chem. Soc* 2004;126:15016–15017. [PubMed: 15547984]

- (4). (a) Pieraccini S, Masiero S, Pandoli O, Samori P, Spada GP. *Org. Lett* 2006;8:3125–3128. [PubMed: 16805568] (b) Ghossoub A, Lehn JM. *Chem. Commun* 2005;46:5763–5765.
- (5). For examples of discrete coordination-driven assemblies that reversibly interconvert by varying the ratio of metal to ligand see a-b; for those that interconvert by changing the solvent see c-d. (a) Hiraoka S, Yi T, Shiro M, Shionoya M. *J. Am. Chem. Soc* 2002;124:14510–14511. [PubMed: 12465941]. (b) Harano K, Hiraoka S, Shionoya M. *J. Am. Chem. Soc* 2007;129:5300–5301. [PubMed: 17411034]. (c) Suzuki K, Kawano M, Fujita M. *Angew. Chem., Int. Ed* 2007;46:2819–2822. (d) Provent C, Rivara-Minten E, Hewage S, Brunner G, Williams A. *Chem. Eur. J* 1999;5:3487–3494.
- (6). (a) Davis JT, Spada GP. *Chem. Soc. Rev* 2007;36:296–313. [PubMed: 17264931] (b) Davis JT. *Angew. Chem., Int. Ed* 2004;43:668–698.
- (7). (a) Gubala V, Betancourt JE, Rivera JM. *Org. Lett* 2004;6:4735–4738. [PubMed: 15575673] (b) Gubala V, De Jesús D, Rivera JM. *Tetrahedron Lett* 2006;47:1413–1416.
- (8). (a) García-Arriga M, Hogley G, Rivera JM. *J. Am. Chem. Soc* 2008;130:10492–10493. [PubMed: 18642917] (b) Betancourt JE, Rivera JM. *Org. Lett* 2008;10:2287–2290. [PubMed: 18452304]
- (9). See Supporting Information.
- (10). (a) Cohen Y, Avram L, Frish L. *Angew. Chem., Int. Ed* 2005;44:520–554. (b) Kaucher MS, Lam YF, Pieraccini S, Gottarelli G, Davis JT. *Chem. Eur. J* 2004;11:164–173.
- (11). By comparison **mAGi** in CD₃CN gives $D = (6.430 \pm 0.114) \times 10^{-10} \text{ m}^2 \text{ s}^{-1}$ at 298 K, which corresponds to a hexadecamer with $r_H = 9.96 \text{ \AA}$.
- (12). This represents a 2% difference with the theoretical value of 9,387 Da calculated for **(mECGi)₁₆• 3KI**.
- (13). The Hill coefficient should be viewed not just as a lower end on the number of binding sites in a receptor, but as an “interaction coefficient” that indicates the level of cooperativity in a system. Weiss JN. *FASEB J* 1997;11:835–841. [PubMed: 9285481].
- (14). The use of Hill coefficients as a measure of cooperativity in self-assembly should only be used when all the stepwise constants refer to identical intermolecular processes. Ercolani G. *J. Am. Chem. Soc* 2003;125:16097–16103. [PubMed: 14678002].
- (15). García-Arriga, M.; Hogley, G.; Rivera, JM. Unpublished results
- (16). Chloroform's low relative permittivity ($\epsilon = 4.89$, $E^N_T = 0.259$) favor the formation of ion pairs. This is in contrast with acetonitrile, which is significantly more polar ($\epsilon = 35.94$, $E^N_T = 0.460$) enhancing the activity (and solubility) of individual ions by preventing their association. For more details see SI p. S17 and Reichardt, C. *Solvent and Solvent Effects in Organic Chemistry*. Third ed.. Wiley-VCH; Weinheim: 2003. .
- (17). According to Coulomb's law the energy of an ion pair, K^+/X^- , increases as the interatomic distance decreases. For more details see ref. 9.
- (18). (a) Anslyn, EV.; Dougherty, DA. *Modern Physical Organic Chemistry*. University Science Books; Sausalito: 2006. (b) Dill, KA.; Bromberg, S. *Molecular Driving Forces: Statistical Thermodynamics in Chemistry and Biology*. Garland Science; New York & London: 2002.
- (19). Rivera JM, Craig SL, Martin T, Rebek J. *Angew. Chem. Int. Ed* 2000;39:2130–2132.
- (20). The residence lifetime for the subunits in the outer tetrads of **(mECGi)₁₆**, as determined in CD₃CN by EXSY NMR, is 66.7 s. For more details see Figure S13 and Perrin CL, Dwyer TJ. *Chem. Rev* 1990;90:935–967..
- (21). For a detailed study on the differential affinity for cations in lipophilic G-quadruplexes see: Ma L, Iezzi M, Kaucher MS, Lam YF, Davis JT. *J. Am. Chem. Soc* 2006;128:15269–15277. [PubMed: 17117879].
- (22). The residence lifetime for the potassium cations in the G-quadruplex structure formed by 5'-GMP has been estimated at 250 ms. (a) Wong A, Ida R, Wu G. *Biochem. Biophys. Res. Commun* 2005;337:363–366. [PubMed: 16185663]. (b) Ida R, Wu G. *J. Am. Chem. Soc* 2008;130:3590–3602. [PubMed: 18293981]. (c) Neidle, S.; Balasubramanian, S. *Quadruplex Nucleic Acids*. The Royal Society of Chemistry; Cambridge: 2006. .

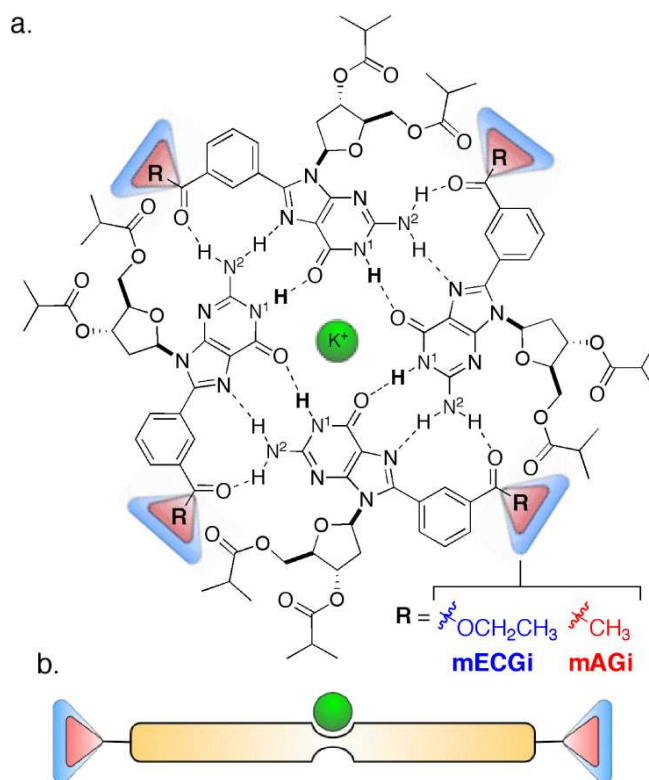


Figure 1. (a, Top view) Chemical structure of the **mECGi** and **mAGi** tetramers and (b, side view) cartoon depiction of the same tetramers. The blue and red triangles represent the differences in steric bulk in **mECGi** relative to **mAGi** respectively.

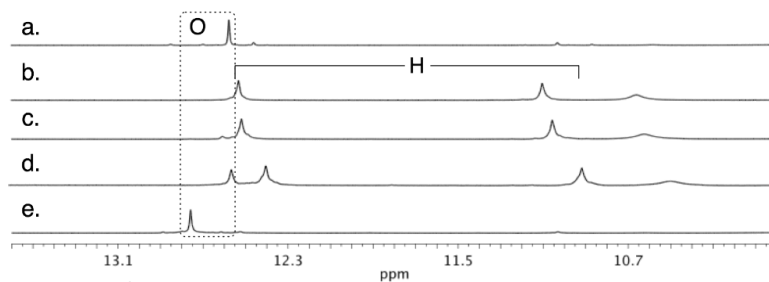
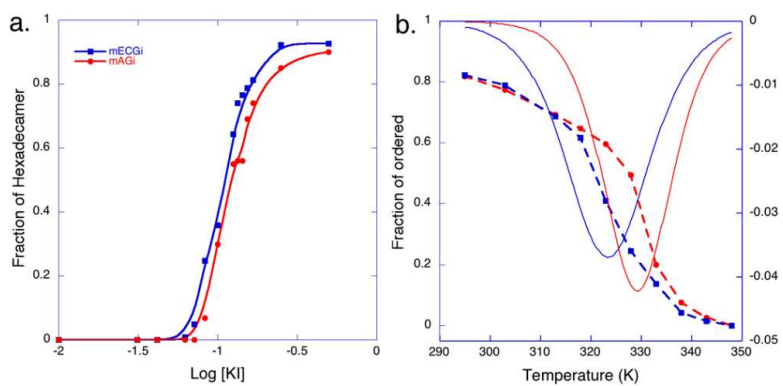


Figure 2. ^1H NMR (500 MHz, 298.2 K) spectra of five samples of **mECGi** (30 mM) in (a) CD_3CN with 0.125 eq. of KI, and with 0.5 eq. of KI using variable $\text{CDCl}_3:\text{CD}_3\text{CN}$ solvent ratios (b) 0:1, (c) 1:1, (d) 4:1, (e) 1:0. The supramolecule exists primarily as $(\text{mECGi})_{16}\cdot 3\text{K}^+$ (**H**, b–d) or $(\text{mECGi})_8\cdot \text{K}^+$ (**O**, a, e). For a full view of all the spectra see Figures S5, S7.⁹

**Figure 3.**

(a) Dose-response curve for the titration of **mECGi** (blue) and **mAGi** (red), 15 mM in CD_3CN .¹⁵ (b) Melting profiles for **(mAGi)₁₆** & **(mECGi)₁₆** (5 mM, 0.5 eq. KI) in CD_3CN as determined by ^1H NMR (500 MHz). The T_m is the inflexion point in the melting profiles as determined by the minimum in the respective first derivative plots.

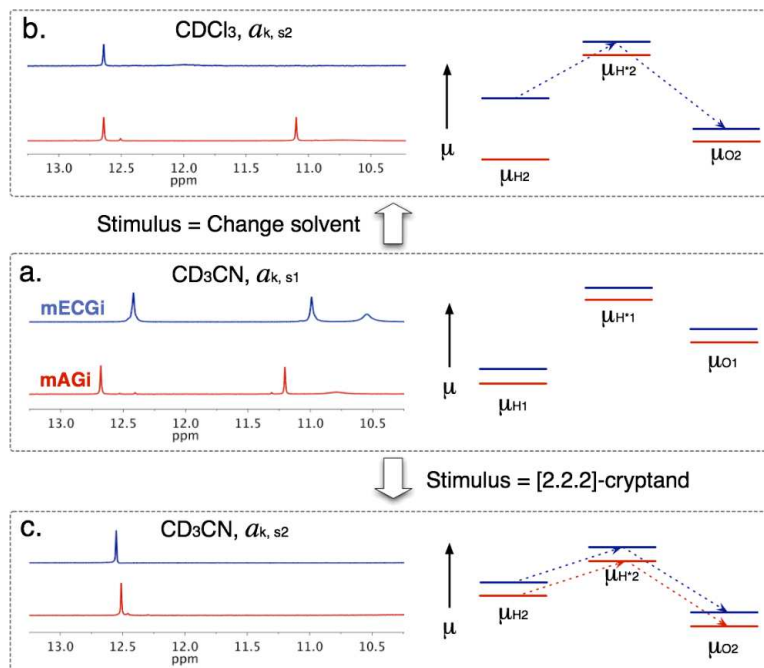
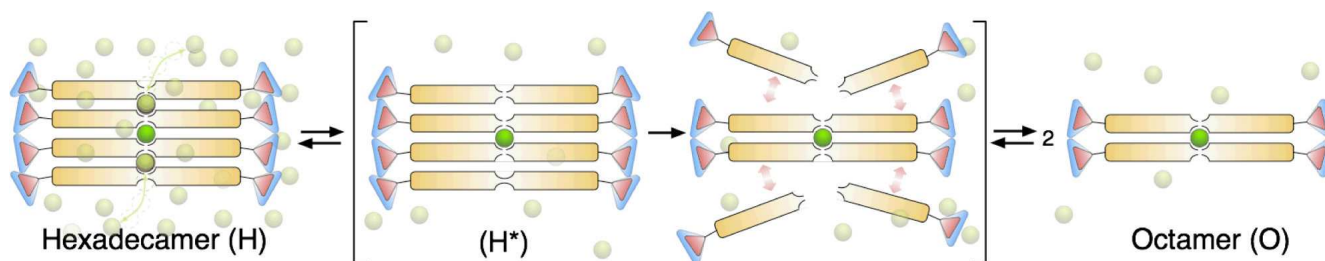


Figure 4. Partial ^1H NMR spectra (500 MHz, 298.2 K) of **mECGi** and **mAGi** in (a) CD_3CN and (b) CDCl_3 . (c) The same as (a) but with 1 eq. of [2.2.2]-cryptand. The peaks in the region of 11–13 ppm correspond to the N^1H and the broad peak at around 10.8 ppm corresponds to the N^2H on the Watson-Crick edge of the guanine moiety. The hexadecamers show a signature of doubled set of resonances due to the two sets of tetrads that are in different chemical environments. (a–c, right) Diagrams illustrating the relative chemical potentials (μ) for the hexadecamers (μ_{H}), putative partially-filled hexadecamer (μ_{H^*}) and octamers (μ_{O}). The dotted arrows indicate that the decay of H is spontaneous under the conditions shown on the left.

**Scheme 1.**

Representation of the solvent-induced switching between a hexadecamer and an octamer. The potassium cations are represented by green spheres in which the more tightly bound potassium cations are darker (inner binding site) and the more weakly bound cations are lighter (outer binding site). H* represents a metastable hexadecamer with empty cation binding sites between the outer and inner tetrads.